한국공작기계학회논문집 Vol.10 No.6 2001. 12.
Transactions of the Korean Society of Machine Tool Engineers

Contour machining error in NC milling process

Chaikwan Namkoong* and I. Yellowley**

Abstract

The comprehensive system analysis for contour milling operation has performed in this study, which combined the each element with proper connectivity into closed loop system, and determined the system response by numerical simulation technique.

The obtained simulated results were then compared with the experimental results from the practical points of view, and so forth, the governing equations were formulated into the estimation model, which predicted the total contour machining error within 25% accuracy. Through the procedural evaluation, it could ascertain the characteristics of generation mechanics in circular contour machining error, and the weight of each factor.

1. Introduction

The contour machining error generated in NC milling process is not only an important factor estimating the quality of manufactured goods, but also a measure of servo system design. However, it is very difficult to analyze the contour machining error because of the complicated correlations between the servo drive system and motion delivering elements, and between cutter and workpiece cutting mechanics. And for this reason, the analysis that only considers the one or two of above factors had been long used.

The problem of reducing path error or individual axis error may be achieved through path preprocessing in which a dynamic model of the machine system is utilized in the path planning process[1-5]. The paper here is, however, concerned with the real time control of error, which is perhaps a more recent activity. from a viewpoint of practice. Several other authors have examined this area, notably Tomizuka[6,7] who has attempted to minimize path errors through the achievement of the command very close to the zero phase lags between the command and actual position of each axis. The essence of the work described by Tomizuka is the use of a compensating filter which attempts to cancel the dynamics of the control loop; it should be evident that this type of approach needs a good knowledge of plant structure and parameters in advance. Additional problems are happened due to physical constraints and nonlinearites; in the case of the previous work by Weck[8] proposing a solution to this problem witch involves placing a low pass filter in front of the controller. The solution proposed by Weck alleviates the amplifier saturation problem and in practice has been shown to lead to

* Dept. of Mechanical Design, Seoul National University of Technology, Seoul, Korea 139-743 (namkoong@duck.snut.ac.kr)
** Dept. of Mechanical Engineering, University of British Columbia, Vancouver, Canada V6T 1Z4

an improved performance in corner tracking.

A rather different approach to the minimization of path error has been introduced by Koren[9,10], who sets out to minimize path errors while still allowing actual individual axis position error. The approach requires the calculation of path error to compensate the individual axis.

The strategy suggested by Koren requires very fast hardware to allow this procedure of cross coupling errors to be achieved in a realistic fashion. The approach proposed by Lee[11] present the performance of the cross-coupled controller that make more precise contour error. The approach taken in the study of Yellowley[12] was intended to allow the possibility of controlling error in real time; even in those cases that constraints such as amplifier saturation were encountered.

In this study, the contour error prediction algorithm was proposed, also the cutting mechanics as well as the errors due to the deflection of tools was considered by simulations then simulated. The simulated results were compared with experimental data to verify the algorithm. Understanding of the contour error in vertical end milling applications is very important for compensation the errors to achieve more accurate parts.

2. Contour error estimation

2.1 Error estimation procedure and method

In order to estimate the contour error, the equations are needed to correlate with the obtained results in procedural manner. As the cutting operation occurs, the calculations are carried out by comparing the result between the increment ΔT. and with the initial conditions given for the nonlinear relationship, the following equation for the cutting coefficient that are collection empirically is shown as:

$$K_{i,k} = C\ D^{\alpha}_{r(k-1)} D^{\beta}_{a}\ f^{\gamma}_{z(k-1)} \tag{1}$$

where i is axis index, and k is iteration index for incremental time.

The equation for a cutter runout is found to be

$$C_{r,k} = C_0 + \sqrt{D_{cx}(k-1)^2 + D_{cy}(k-1)} \tag{2}$$

where Co is geometric initial runout, and D_{ex} and D_{cy} are x, y component of cutter deflection.

Then, the feed velocity vector for each axis is shown as

$$V_{i,k} = V_{i,k-1} + E_{i,k-1} / \Delta T \tag{3}$$

where is change of location at (k-1) respect to k.

Therefore, the feed direction angle α_k becomes

$$\alpha_k = \tan^{-1}(V_{xk} / v_{yk}) \tag{4}$$

Where V_{xk} and V_{yk} are x, y component of feed velocity. And, feed rate per tooth at k^{th} step is

$$f_{z,k} = f_{z(k-1)} + \Delta D_{cx,(k-1)} \sin\ \alpha_k \tag{5}$$

In Fig.1 every m^{th} section at n^{th} flute is said to emerged in the rotational angle mn,k and uncut chip thickness then becomes

$$h_{mn,k} = f_{z,k} \sin\phi_{mn,k} + C_{r,k} \tag{6}$$

And the cutting force can be derived as below

$$F_{i,k} = \sum_{n}\sum_{m} \delta_{mn} K_{i,k(mn)}\ \ h_{mn,k} \Delta W \tag{7}$$

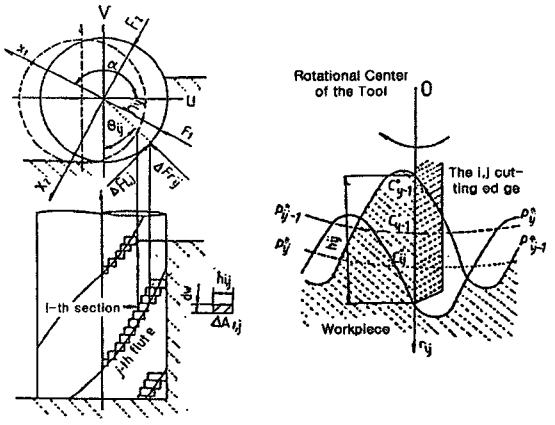

Fig. 1 Force computing model

where ΔW is the axial increment of cut and δ_{mn} is delta function of cutting zone.

The equivalent load torque is

$$T_{1,mc(ik)} = \frac{1}{2\pi\eta} F_{i,k} + T_{sfk} \tag{8}$$

Consequently, the contour servo control error from above equations becomes

$$e_{si,k} = e_{i,k} + E_{ssi,k} \tag{9}$$

where

$$E_{ssi,k} = \frac{R \cdot T_{1,nc(i,k)}}{k_t \cdot k_c \cdot k_a} \tag{10}$$

$$e_{i,k} = V_{i,k}\left\{\frac{1}{K_i} - S_i \; e^{-T/2\tau_i} \sin\left(\frac{T}{S_i} - \gamma_i\right)\right\} \tag{11}$$

and where $S_i = \dfrac{2\tau_i}{\sqrt{4K_i \cdot \tau_i}}$

The first term of the equation (9) is the expected error proportional to velocity, and the second term indicates the friction-induced error.

The deflection of cutter and workpiece are also defined as

$$D_{ci,k} = \frac{F_{i,k}}{Q_1} \;\; and \;\; D_{wi,k} = \frac{F_{i,k}}{Q_2} \tag{12}$$

where Q_1 and Q_2 are stiffness of materials.

Therefore, metal removal rate during contour cutting can be expressed by

$$E\Sigma,\; k = (D_{cx,k} + D_{wx,k} + D_{sx,k})\cos\alpha_k + (D_{cy,k} + D_{wy,k} + D_{sy,k})\sin\alpha_k \tag{13}$$

The calculation is repeated at each increment ΔT, and the updated values of the contour error simulation are shown in Fig.2 where step- by-step procedural approaches were outlined for the prediction of contour error estimation.

The exponential acceleration and deceleration of the movements are represented by the equation (14), where circular cutting or corner removal is a function of axis of motion, changing of directions, and stop and starting.

$$V_{ik} = V_{i,k-1} \pm V_{0i} e^{-\beta t} \Delta T \tag{14}$$

And automatic acceleration or deceleration model of the system is illustrated in Fig.3 that eventually arrives at the stable condition.

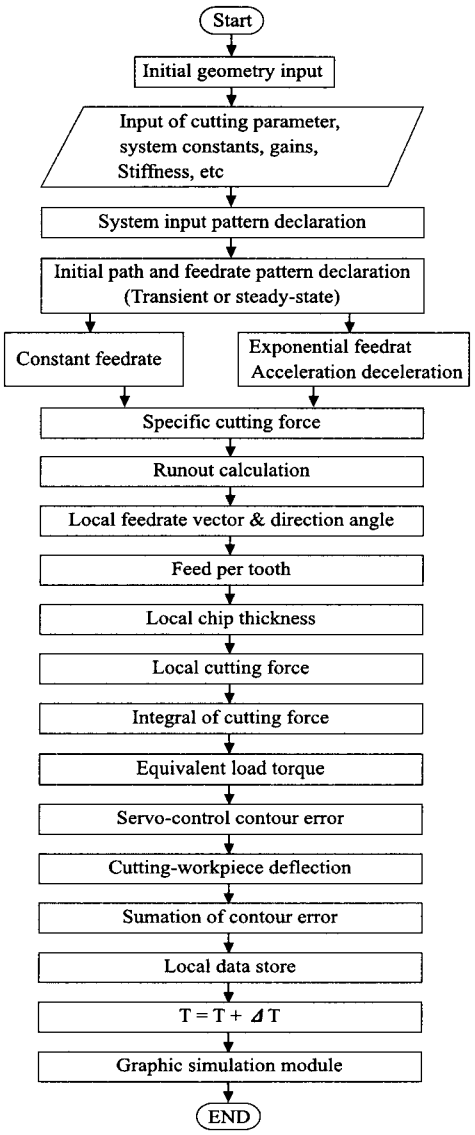

Fig. 2 Estimation procedure of contour error

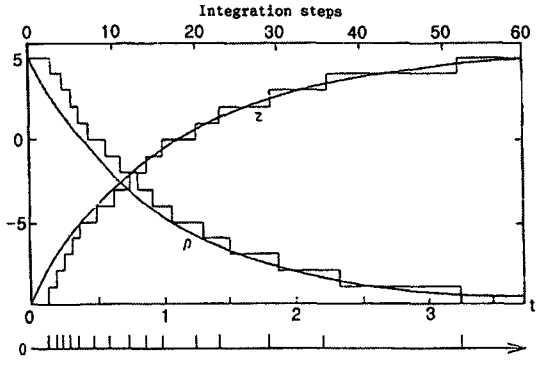

Fig.3 Automatic acceleration / deceleration model of feedrate

2.2 Simulation results and discussion

In this section, the simulation data are investigated using a graphic simulation module (GRAFIT). First, the system factors (constants) and gain factors are obtained based on the NC machine used in the experiment. The end-mill parameters used in the calculation were based on the HSS material by Kops[14], which is shown in Table 1.

From the table, we obtain $E_w I_w = 9.55 \times 10^8$ kg$_f$/mm^2(equivalent stiffness coefficients for workpiece) as well. The down-milling operation was simulated using 16 mm diameter endmill to acquire contour errors. The calculated contour errors are depicted in Fig.4 and 5.

In Fig.4, two fluted end-mill was used to calculate values

Table 1 Stiffness of end mill and cutting constants

End mill diameter (mm)	Loading condition		Max. deflection (mm)	
	F (kgf)	Da (mm)	Dci (mm)	
12.70	59.6	19.05	86.2	
	16.0	12.70	26.0	
	44.9	12.70	73.3	
18.14	100.0	28.58	25.7	
	51.6	28.58	13.8	
	70.3	19.05	26.6	
	34.3	9.53	15.8	
(kg$_f$/mm^2)	C	α	β	γ
K_T	175	-0.161	0.043	-0.345
K_R	121	-0.079	-0.437	-0.344
K_Z	10	-0.321	0.187	-0.685

where Fig.4(a) illustrates the cutting force and Fig.4(b) illustrates the contour error, servo counter error, and workpiece deflection errors in x and y directions. When we investigated the simulation results, the cutting force graphs

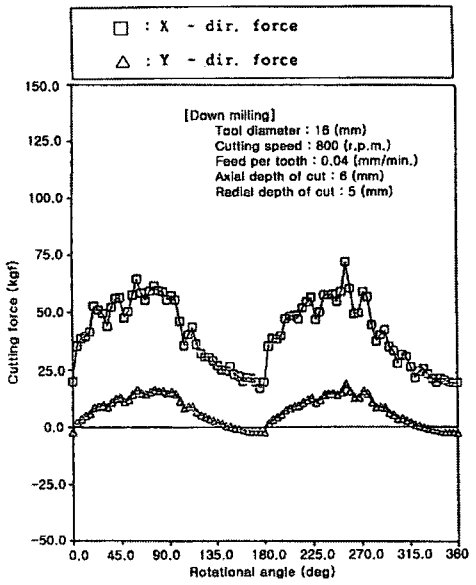

(a) Cutting force

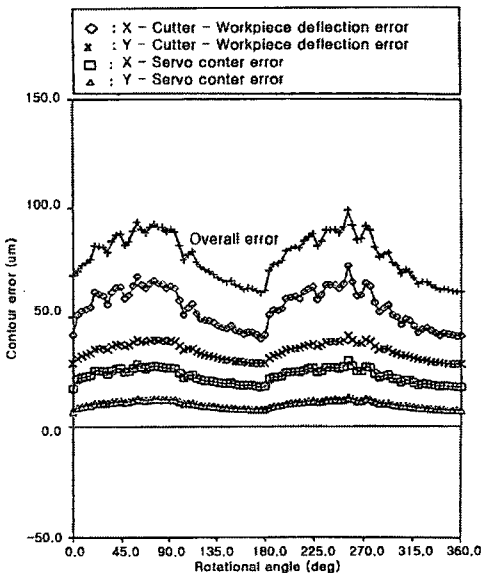

(b) Contour error

Fig. 4 Simulation results of contour error for 2-fluted cutter

show the same trend as the other force measurements; however the simulation data contain uncertain noise. The noise may be occurred due to the runout factor that was considered in the calculation at each increment of time, and consequentially changed the chip thickness. The contour error also exhibits similar trend as the force measurements.

The servo error graph shows significantly less noise than the workpiece deflection error graph with 3 to 5 times more noise. In Fig.5, four -fluted endmill cutter was used. From the first graph, the four major peaks are depicted for every one revolution and the noise has much decreased compared to the two-fluted cutter simulation.

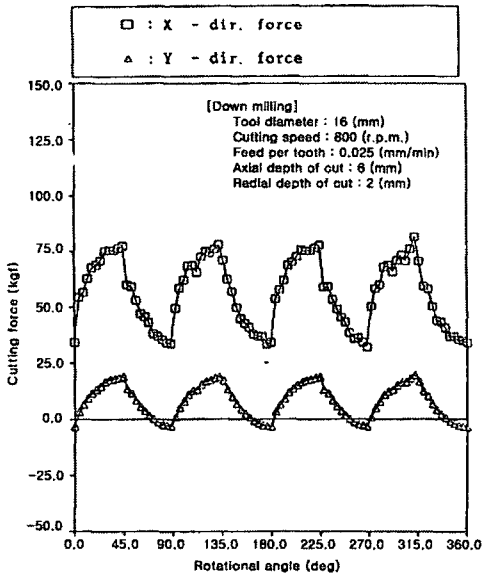

(a) Cutting force

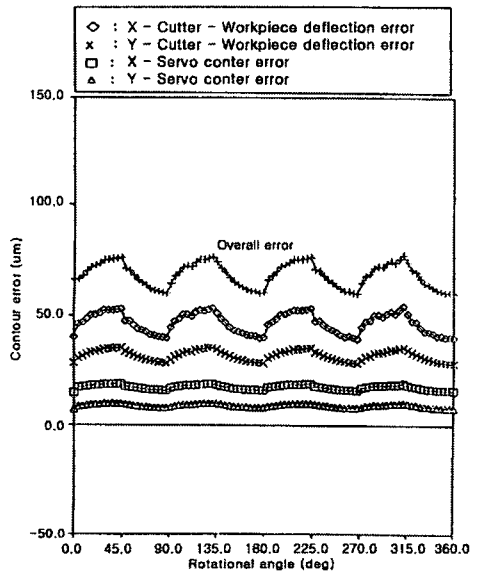

(b) Contour error

Fig. 5 Simulation results of contour error for 4 -fluted cutter

3. Experimental setup and procedures

In this study, we have used structural carbon steel SM45C as a workpiece, and small holes were made to facilitate the clamping fixture on the milling machine. In addition, machinable wax workpiece was also used to investigate the effects of the stiffness of the materials and loads due to cutting forces. The mechanical and chemical properties of test pieces are shown in Table 2.

Table 2 Mechanical and chemical properties of testpieces

Test material	Mechanical properties				
SM45C	Hardness -tion (HB)	Tensile strength (kg_f/mm^2)	Elonga strength (%)	Yield of area (kg_f/mm^2)	Reduction (%)
	157	71.2	18.5	36.43	31.4
	Chemical composition (%)				
	C	Si	Mn	P	S
	0.45	0.31	0.75	0.016	0.012
Machinable wax - IPCO					

The end-mills used in the experiment were both two and four fluted 16 mm diameter with 30 degrees helix angle and they are made up of high-speed steel (SKH9) material. The endmill stiffness value was based on Kop's model[14] shown in Table 1.

The strain gauge for a force measurement system (Lebow ETN6423) was used to measure the cutting forces where the strain gauge signal is amplified through an A/D converter which is then fed into a PC to acquire the data. The sampling rate was 10 kHz.

The contour error was measured by a computer measure-

ment machine (CMM Rank Taylor Hobson RTH TR250 model) roundness tester for the machined test pieces. The accuracy of the machined surface finish measurement was approximately 0.1 mm for 3D measurements and the 5 mm diameter probe was used to measure roundness.

The experimental cutting conditions are shown in Table 3 for the machinable wax, upmilling and down-milling.

Table 3 Cutting conditions used in experiments

No	Group	Cutting speed (rpm)	Feed (mm/tooth)	Axial depth of cut (mm)	Radial depth of cut (mm)
1	Up milling	800	0.04	6	5
2	Down milling	800	0.04	6	5
3	Machinable wax	800	0.04	6	5

4. Results and discussion

In this section, the simulation results are compared with the experimental data during the period of one revolution of the cutter.

Fig.6 is the comparison of the two fluted cutter for down-milling operations, where Fig.6(a) depicts the cutting force and (b) is contour error. The cutting force data were converted using an A/D converter for every 10kHz sampling and contour error was measured using a 3D CMM machine. From fig.6, the simulation data show some non-uniform oscillation due to noise. Unlike the simulation data for this case, the experimental force shows smooth curves. consequently, the experimental and the simulation data matches nicely each other. The simulation cutting force values are higher by 20kgf than those of experiments in some instances and contour error deviation is about 10mm. The workpiece deflection error is greater than servo contour error as shown in Fig.6(b). The servo error has approximately 30% portion of the overall error.

Fig.7 is an up-milling operation for the same cutting conditions as Fig.6. The cutting force diagram shows negative values compared with the down-milling operation case. Furthermore, there is fluctuation, approximately 7kgf deviations, in X direction, and approximately 20kgf deviates compared from the down-milling operation. The similar behaviour was observed with the cutting force diagram also occurs in the contour error diagram, as shown in Fig.7(b). Maximum value become about 40% less then the down-milling. In addition, for the case of up-milling operation, the contour error fluctuates less than down-milling. The similar trend can be also observed for four fluted cutter case as well, which is not shown.

Following the contour error results, feed velocity vectors are investigated for the simulation and experimental data, and the equations are shown as

$$Vx = R\ \omega\ \cos(\omega t)$$
$$Vy = R\ \omega\ \sin(\omega t) \tag{15}$$

The large value of radius of the workpiece

was used for cutting feed. x and y axis servo feed velocities were used from Equation (14) for each iteration.

$$V_{i,k} = V_{i,k-1} \pm V_{oi} e^{-0.5t} \Delta t \tag{16}$$

The 0.5sec increment was modeled for each index (i.e., for i = x, y) of feed velocity. Radial contour error, which is time dependent, was calculated as follows

$$R(t) = \sqrt{x_0(t)^2 + y_o(t)^2} \tag{17}$$

Prior to calculations of the contour error, errors from NC servo drive were needed to investigated. For the initial calculation, external loads were neglected then considered at the later stage. Numerical calculation result of servo error in NC feed drive system is illustrated in Fig.8.

For an investigation of the external load on the NC feed drive, a machinable wax workpiece was machined with the same condition as the steel workpiece to determine the effects of the external loads. This investigation is illustrated in Fig.9.

When we compare the simulations and experimental results, the overall circular shape matches each other. The simulation calculations deviates about 25% from the exper-

imental results which may be due to other factors. The comparison of circular contour error between calculation and experiment is represented in Fig.10.

Overall comparison between fig.9 and 10 shows the similar results. Up-milling value shows about 1.5 - 2 time of the circular radiation error in negative direction. The up-milling

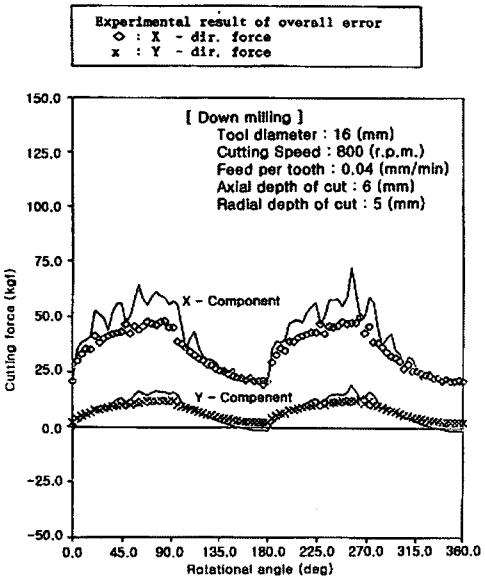

(a) Cutting force

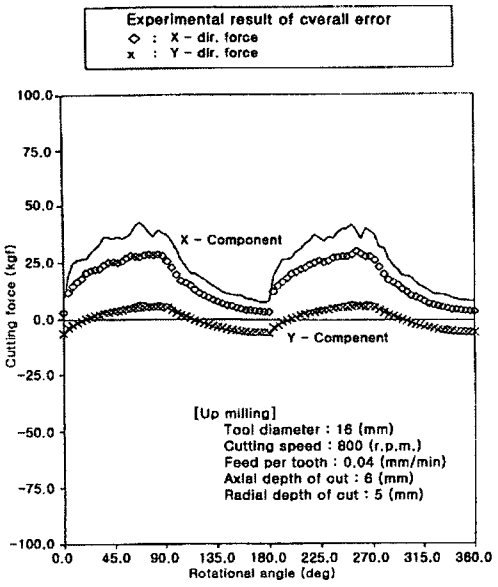

(a) Cutting force

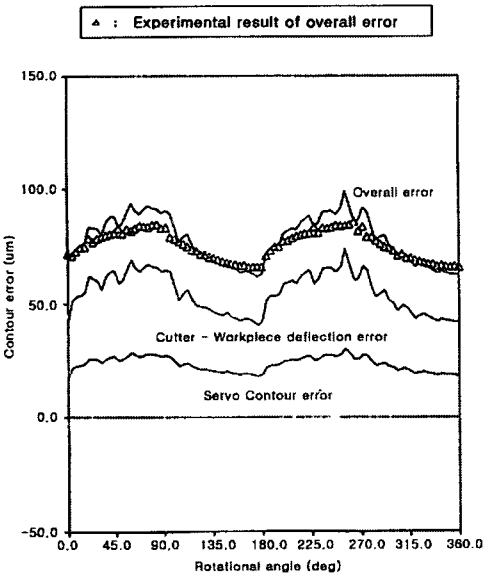

(b) Contour error

Fig. 6 Comparison of cutting force and contour error down milling

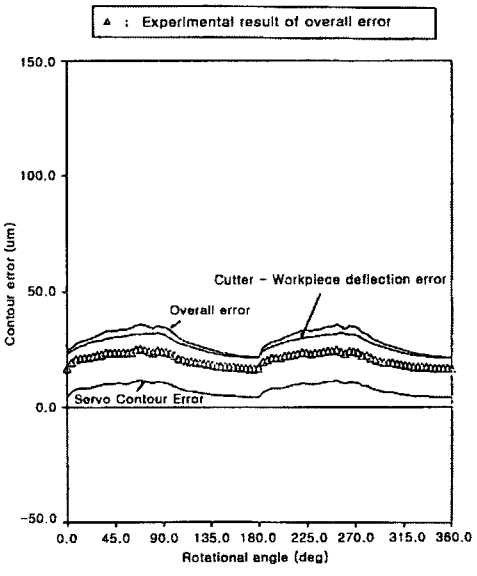

(b) Contour error

Fig.7 Comparison of cutting force and contour error up milling

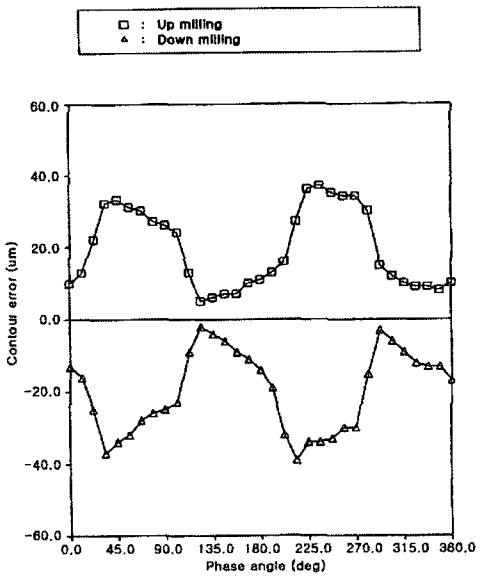

Fig. 8 Numerical calculation result of servo error in NC feed drive system

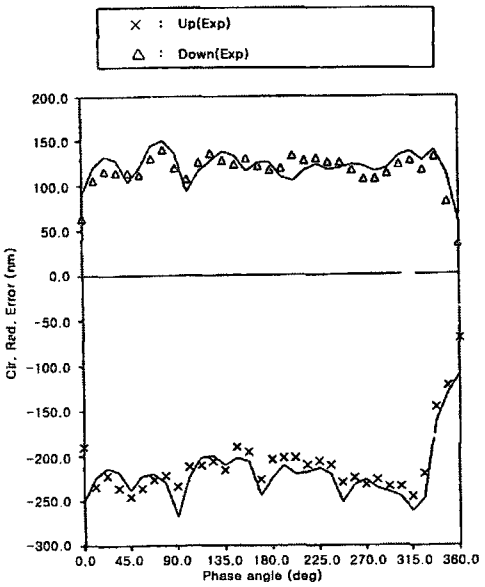

Fig.10 Comparison of circular contour error between calculation and experiment

contour error between the simulation and the experimental results show good match with each other. However, errors in down-milling experimental data are slightly more than those of simulated data.

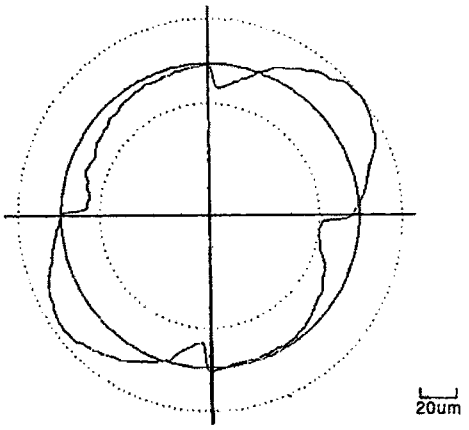

No	Group	Cutting speed	Feed (mm/tooth)	Axial depth of cut (mm)	Radial depth of cut (mm)
3	Machinable wax	800	0.04	6	5

Fig. 9 Curve of roundness error in the machining of machinable wax

This is mainly due to cutter behaviour in down-milling operation. The deviation increases significantly either at 0 or 360 degrees of tool rotation. The behaviour can be explained by considering that when the initial tooth enters the workpiece, which, the impact causes momentary vibration, which explains the outcome compared with the up-milling operation.

5. Conclusion

This study addresses the comprehensive analysis on the contour error due to the servo errors as well as error caused by dynamic behaviour of the system. The simulation results were then compared with the experimental data to come up with an effective model, which can be used to calculate the contour error in milling operations. The summary of this study follows:

During this simulation and experimental investigation process, it is found that the biggest factor affecting the contour error in milling analysis is due to deflection of cutter, which contributes to approximately 50 to 80% of overall error.

NC servo error contributes approximately 20 to 50% of the overall contour error. The servo error directly affects the chip thickness that causes the fluctuation of cutting forces.

When circular contour error is calculated the new estimation model considering the acceleration and deceleration effects of the feed drive units is approached to improve the matching between estimation and experimental results.

Simulated contour error results were matched with the experimental data by considering cutter runout, chip thickness, and changing of the feed velocity.

Nomenclature

B	Motor constant
C	Cutting constant
Cr	Cutter runout
D_a	Axial depth of cut
E_cI_c	Cutter stiffness (N-m^2)
E_wI_w	Workpiece equivalence stiffness (N-mm^2)
F_c	Cutting force in X and Y direction
F_f	Ball screw feed force (N)
f_z	Feed rate per tooth (mm/tooth)
f_m	Feed per minute (mm/min)
h	Un-deformed chip thickness
i	Axis index
J_m	Motor inertia (kgm^2)
k	Iteration index for incremental T
K_a	Amplifier gain
K_b	Bearing stiffness (N/mm)
K_c	Converter gain (V/pulse)
K_g	Gear ratio
K_i	$C\ D_{r(k-1)}^{\alpha}\ D_a^{\beta}\ f_{z(k-1)}^{r}$
K_n	Nut stiffness (N/mm)
K_s	Ball screw stiffness (N/mm)
K_t	Motor torque (Nm/A)
K_v	Motor constant (VS/rad)
L	Length of cutter (mm)
N	Rotational speed (rpm)
R	Motor resistance (Ω)
T_m	Motor friction torque (N mm)
v	Velocity
W	Weight of Table and workpiece (kg)
X_0	Vibration movement
z	Number of flutes
μs	Friction coefficient
η	Friction between table and ball screw
φ	Rotational angle
φ_a	Axial rotational angle
φ_r	Radial rotational angle
φ_c	Rotational angle due to cutting tooth
ΔW	Changing of width of cut
δ_{mn}	Delta function due to cutting area
w	Natural frequency
$\alpha\ \beta\ \gamma$	Cutting constants
ΔT	Incremental time

References

(1) H.A. Park. "Adaptive matching and preview controllers for feed drive systems". ASME Trans. J. Engng Ind. Vol.113, pp 316-320, 1991.

(2) W.J Lee, T.S Yun and S.I. Kim. "Development of a machining error estimation system for vertical lathes with structural deformation and geometric error". Journal of the Korea Society of Machine Tool Engineers. Vol 8, No 3, pp 15-21, 1999.

(3) J.Y. Ahn and S.C. Chung. "Modeling and compensatory control of thermal error for the machine origin of machine tools". Journal of the Korea Society of Machine Tool Engineers. Vol. 8, No. 4, pp 19-28, 1999.

(4) T.I. Seo and Y.W. Cho. "Study of machined surface error compensation for autonomous manufacturing system". Journal of the Korea Society of Machine Tool Engineers. Vol. 9, No. 4, pp 75-84, 2000.

(5) B.H. Kim. "Precision machining characteristics in ball-end milling of sculptured surfaces". Journal of the Korea Society of Machine Tool Engineers. Vol. 10, No. 1, pp 78-87, 2001.

(6) M. Tomizuka. "Zero phase error tracing algorithm for digital control". ASME Trans. J. Dyn. Syst. Meas. Control Vol. 109, pp 65-68, 1987.

(7) J. Buttler, B. Haack and M. Tomizuka. "Reference input generation for high speed coordinated motion of a two axis system". ASME Trans. J. Dyn. Syst. Meas. Control Vol. 113, pp 67-74. 1991.
(8) M. Weck and G. Ye. "Sharp corner tracking using the IKF control strategy". Ann. CIRP Vol. 39, pp 437-441, 1990.
(9) Y. Koren. "Cross-coupled biaxial computer control for manufacturing systems". ASME Trans. J. Dyn. Syst. Meas. Control Vol. 102, No. 4, pp 265-272, 1980.
(10) Y. Koren and C.C. Lo. "Variable gain cross-coupling controller for contouring". Ann. CIRP Vol. 104, pp 371-374, 1991.
(11) J.H. Lee and S.H. Yang. "A new contour error model for cross-coupled controller in CNC machine tools". Journal of the Korea Society of Machine Tool Engineers. Vol. 9, No. 6, pp 152-157, 2000
(12) I. Yellowley and R.J. Seethaler, "The regulation of position error in contouring systems". Int. J. Mach. Tools Manufact. Vol. 36, No. 6, pp 713-728, 1996.
(13) I. Yellowley and P.R. Pottier. "The integration of process and geometry within an open architecture machine tool controller". Int. J. Mach. Tools Manufact. Vol. 34, N0. 2, pp 277-293, 1994.
(14) L. Kops and D.T. Vo. "Determination of the equivalent diameter of machinability evaluation using a workpiece model". Ann. CIRP vol. 39, pp 93, 1990